

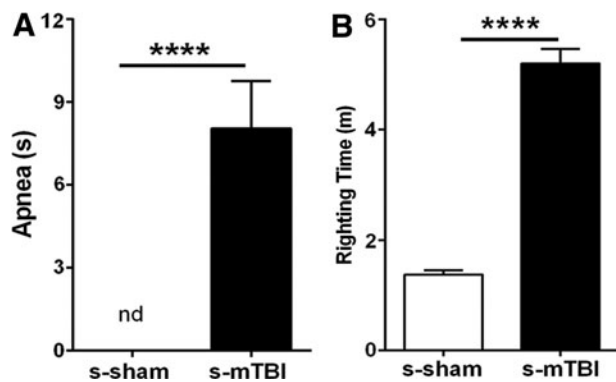
Supplementary Data

Supplementary Materials

Single-injury methods

A single-impact (s-mTBI) model has been previously characterized.²⁹ Mice and methods for anesthesia and stereotaxic procedures were the same as described for the repetitive impact model.

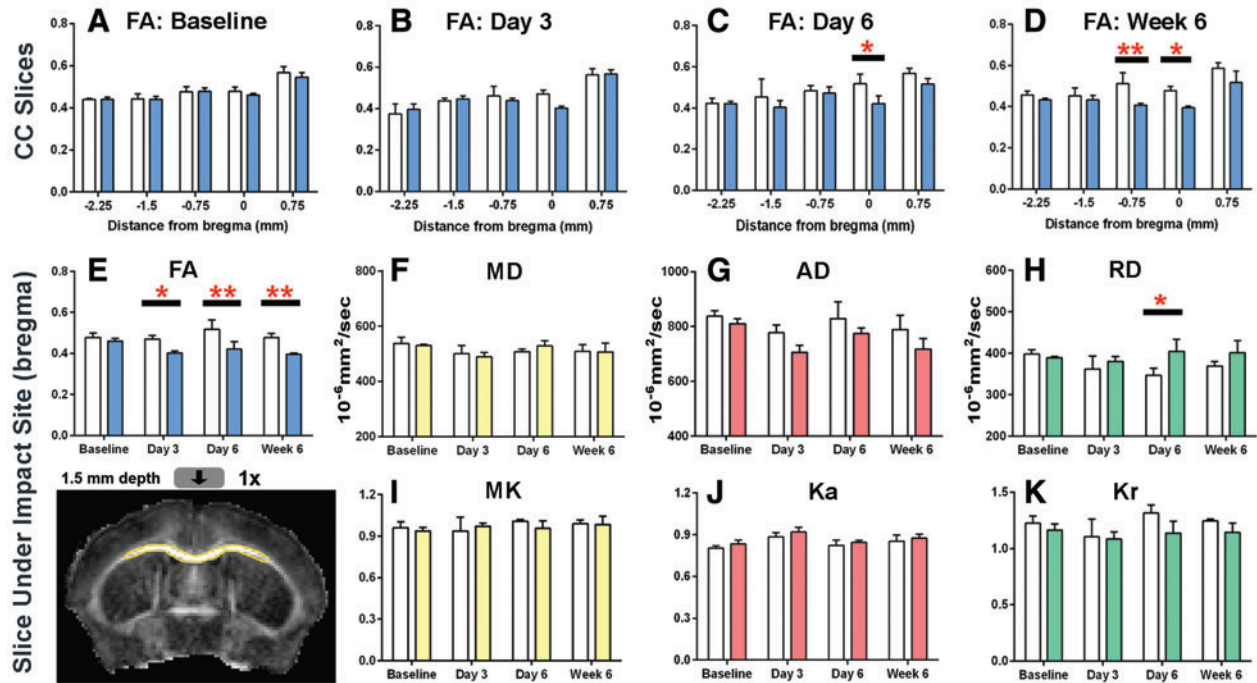
For s-mTBI, the scalp was incised along the midline to expose the skull, and a 3-mm-diameter tip was used to impact the skull at bregma (velocity set at 4.0 m/sec; depth of 1.5 mm; dwell time of 100 ms). Sham mice underwent identical procedures without receiving impacts. The single-injury study included 27 s-mTBI mice and 27 s-sham mice.



SUPPLEMENTARY FIG. S1. Post-surgical data for single mild traumatic brain injury (s-mTBI). Apnea was not detected (nd) after the sham procedure, but apnea duration was significantly increased after the impact in s-mTBI mice (A). The righting reflex time is significantly delayed in injured versus sham mice (B). Values are mean \pm standard error of the mean; $n=27$; **** $p < 0.0001$.

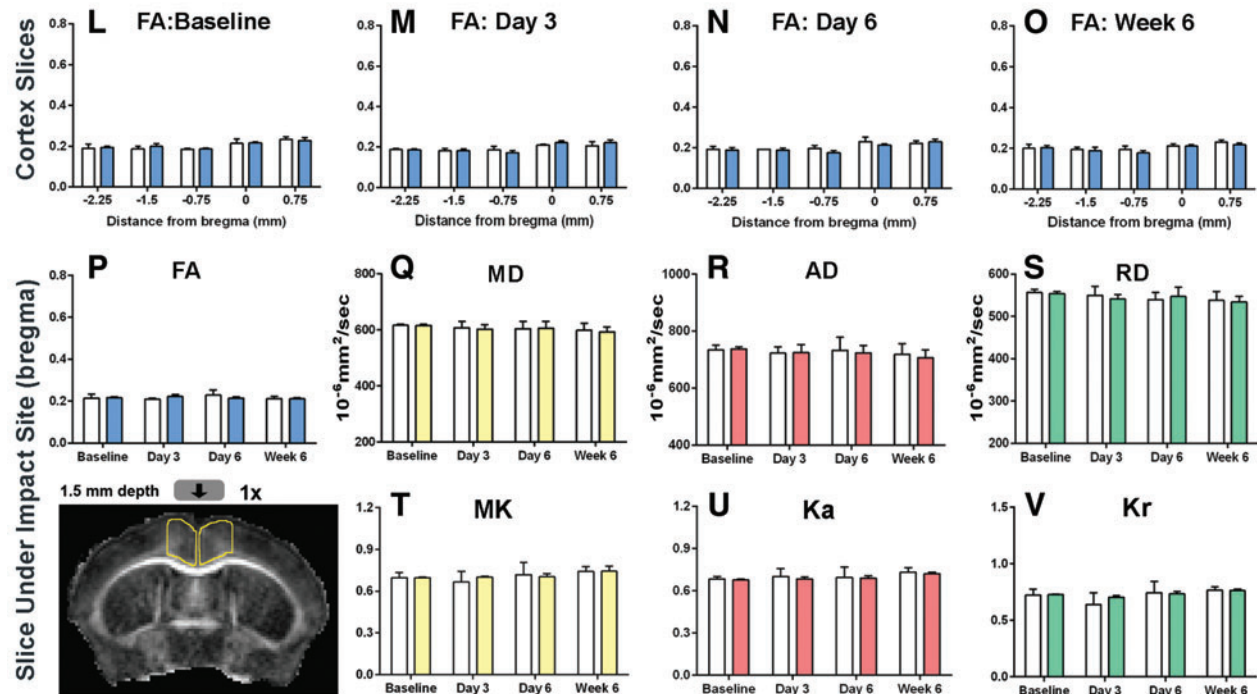
Single mTBI (s-mTBI): Corpus Callosum (CC)

white bars = s-sham; colored bars = s-mTBI

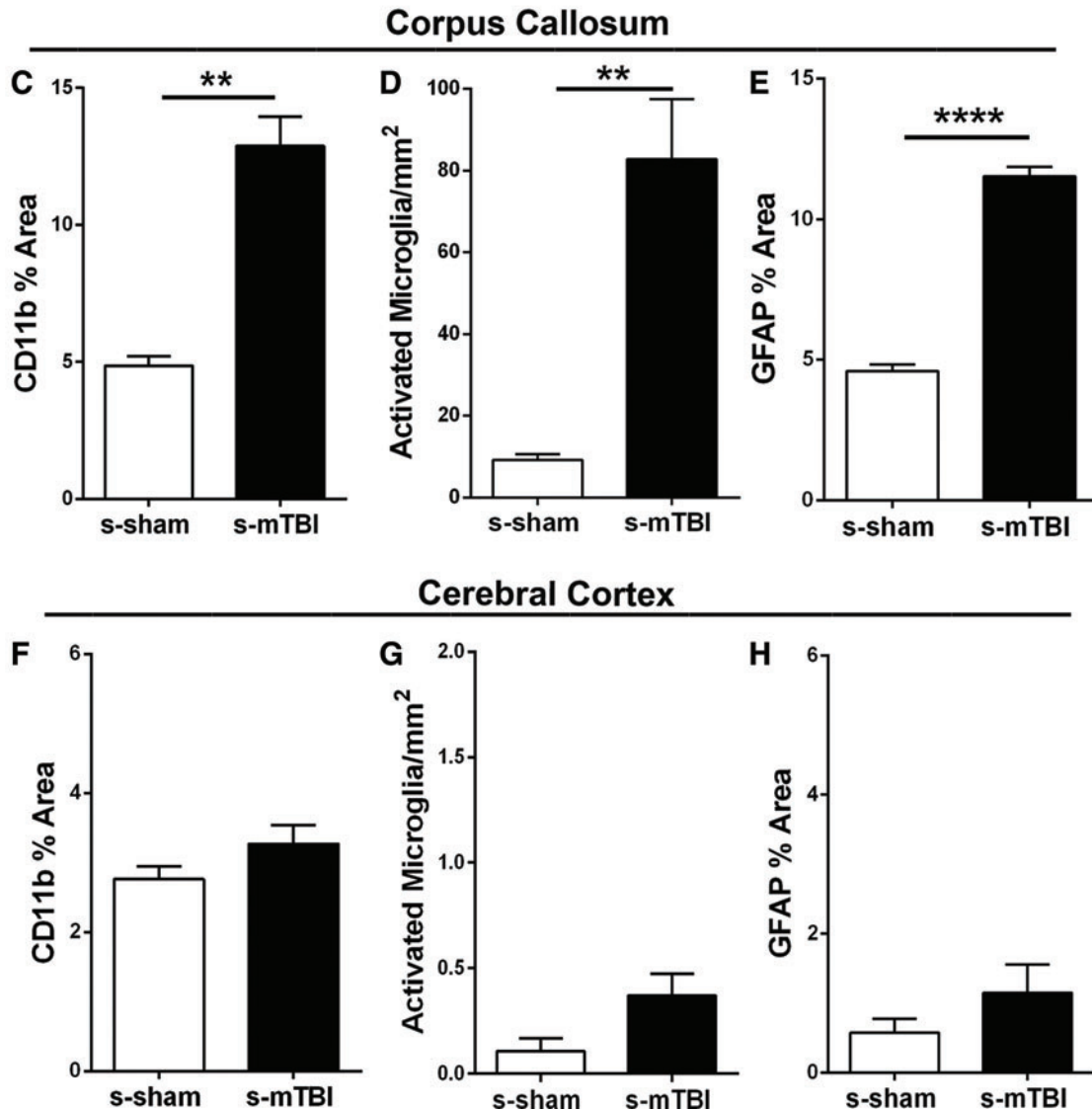
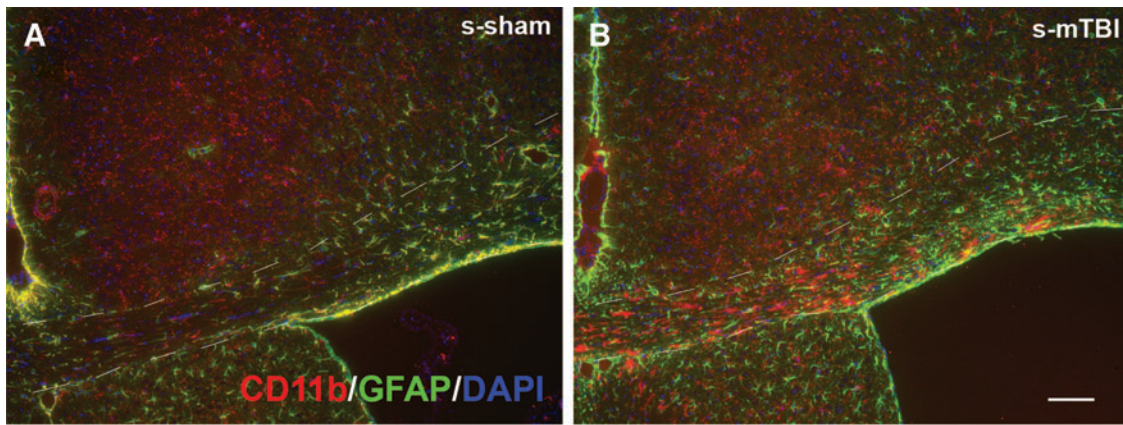


Single mTBI (s-mTBI): Cerebral Cortex

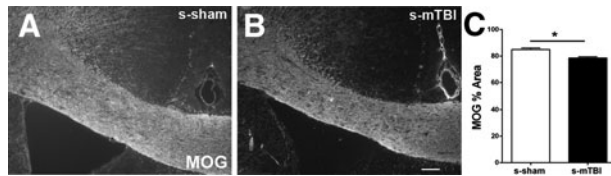
white bars = s-sham; colored bars = s-mTBI



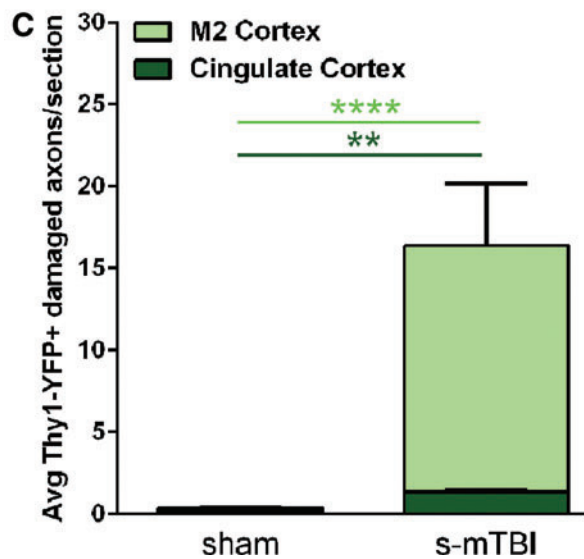
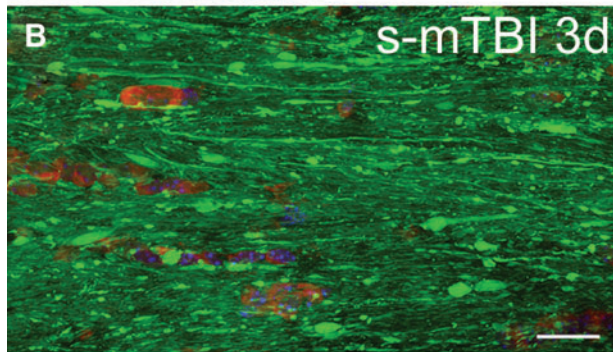
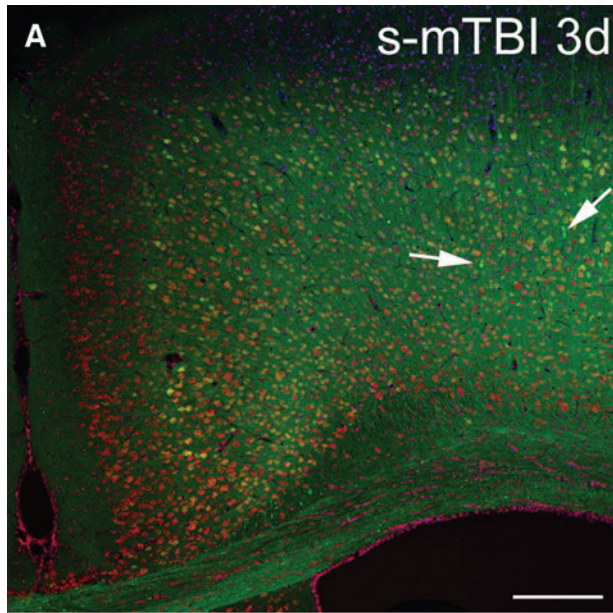
SUPPLEMENTARY FIG. S2. Diffusion imaging results for single mild traumatic brain injury (s-mTBI). (A–K) DTI (A–H) and DKI (I–K) analysis of corpus callosum (CC) region outlined in yellow on upper image. (L–V) DTI (L–S) and DKI (T–V) analysis of medial cerebral cortex region outlined in yellow on the lower image. Each region is shown at the coronal level containing the anterior commissure, which is under the impact site at bregma. s-sham and s-mTBI mice were scanned as yoked pairs with all mice being scanned at four time points—baseline (BL) and post-injury at 3 days, 6 days, and 6 weeks. Five coronal slices (one rostral to bregma, one at the coronal level of bregma=0, and three caudal to bregma) were analyzed. (A–D) FA values in the CC showing all five coronal slices with locations noted as relative to bregma. A significant reduction in FA was noted in s-mTBI mice only at the bregma level at day 6 (C) and spread to include the adjacent caudal slice at week 6 (D). (E–K) CC values in the individual coronal slice at bregma are shown across time points for the full set of parameters analyzed—diffusion tensor imaging (FA, MD, AD, and RD) and diffusion kurtosis imaging (MK, K_a , and K_r). FA was significantly lower in the CC of s-mTBI mice compared to matched sham mice at each post-injury time point (E). Injury decreased AD values, but no time point reached significance on post-hoc analysis (G). RD values also show an overall injury effect and a significant increase at 6 days (H). (L–V) Matching analysis of the medial cortex shows a lack of effect from the single injury. Values are mean \pm standard deviation, $n=3$ for each condition and time point; * $p<0.05$; ** $p<0.01$. AD, axial diffusivity; FA, fractional anisotropy; K_a , axial kurtosis; K_r , radial kurtosis; MD, mean diffusivity; MK, mean kurtosis; RD, radial diffusivity; s-sham, single sham.



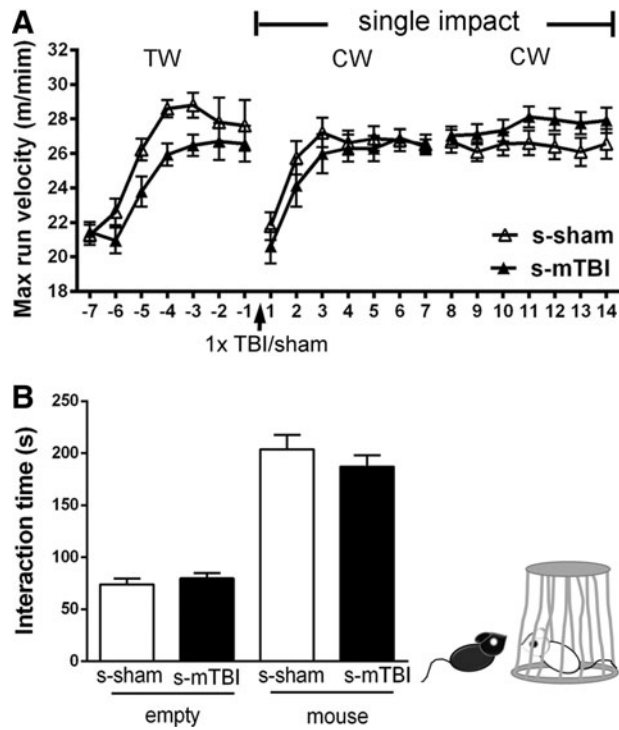
SUPPLEMENTARY FIG. S3. Neuroinflammation in the corpus callosum and cortex for single mild traumatic brain injury (s-mTBI). (A and B) Immunohistochemistry was used to detect microglia/macrophage cells with CD11b and astrocytes with GFAP in mice perfused after the final imaging scan, that is, 6 weeks post-injury or sham procedure. Microglia/macrophage activation and astrogliosis was most evident in corpus callosum after s-mTBI, as shown by the extent of GFAP immunolabeling and the increased intensity of CD11b immunolabeling in cells with a hypertrophic cell body and thickened processes (B) compared to the corpus callosum in s-sham mice (A). (C–E) Quantitative analysis shows that s-mTBI mice exhibit a significant increase in microglial activation in the corpus callosum relative to sham control (C and D). Similarly, astrogliosis in the corpus callosum was significantly increased after s-mTBI (E). (F–H) In contrast, the cortex did not show an increase of microglia activation (F and G) or astrogliosis (H) after s-mTBI. Dashed lines outline the corpus callosum. Values are mean \pm standard error of the mean; $n=3$; scale bar = 50 μm ; ** $p < 0.01$; **** $p < 0.0001$. DAPI, 4',6-diamidino-2-phenylindole; GFAP, glial fibrillary acidic protein; s-sham, single sham.



SUPPLEMENTARY FIG. S4. s-mTBI (single mild traumatic brain injury) resulted in demyelination in the corpus callosum at 6 weeks post-injury. (A and B) Immunohistochemistry for myelin oligodendrocyte glycoprotein (MOG) was used to study myelination status post-imaging after s-mTBI (B) or sham procedure (A). (C) Quantification of MOG showed a small, but significant, decrease in the area of MOG immunolabeling in the corpus callosum after s-mTBI. Values are mean \pm standard error of the mean; $n=3$; scale bars = 50 μ m; * $p < 0.05$. s-sham, single sham.



←
SUPPLEMENTARY FIG. S5. Thy1-YFP-16 mice show axonal pathology in the cortex and corpus callosum after single mild traumatic brain injury (s-mTBI). **(A)** Thy1-YFP (green) shows labeling of neurons throughout the cortex along with axons projecting through the corpus callosum in mice perfused 3 days after s-mTBI. Nissl staining (red) of the cytoplasmic rough endoplasmic reticulum along with DAPI nuclei counterstaining (blue) shows the overall cortical cytoarchitecture, which is not markedly disrupted in s-mTBI mice. Arrows point to examples of swollen segments of damaged axons. **(B)** Thy1-YFP (green) labeled the numerous swollen axonal segments observed in the corpus callosum of s-mTBI mice. Red=Nissl; blue=DAPI. **(C)** Quantification of damaged axonal profiles (swollen, axonal bulbs, and varicosities) labeled with Thy1-YFP in the cingulate and M2 motor cortices that comprise the region of interest in the medial cortex for DTI/DKI analyses. A significant increase of damaged axons was observed in the s-mTBI group compared to sham control. Values are mean ± standard error of the mean; n=3; 3–9 sections per animal. ** $p < 0.01$; **** $p < 0.0001$. Scale bars A=200 μm ; B=20 μm . Avg, average; d, days; DAPI, 4',6-diamidino-2-phenylindole; DKI, diffusion kurtosis imaging; DTI, diffusion tensor imaging.



SUPPLEMENTARY FIG. S6. No social deficits were observed after single mild traumatic brain injury (s-mTBI). The mice were assessed for motor and social tasks related to functions of cortical regions under the impact site at bregma and corresponding areas of the corpus callosum. (A) The cohorts ($n = 12$ per condition) did not show differences in any phase on the training or complex wheel after s-mTBI. (B) A three-chamber sociability test was further employed to test social behavior at 3 weeks after mTBI. The s-sham mice spend the majority of time interacting with the carrier containing a stranger mouse rather than the empty carrier. No difference was observed after s-mTBI. Values are mean \pm standard error of the mean; $n = 12$. s-sham, single sham.